All graphene electromechanical switch fabricated by chemical vapor deposition

Citation: Milaninia, Kaveh M., Marc A. Baldo, Alfonso Reina, and Jing Kong. "All Graphene Electromechanical Switch Fabricated by Chemical Vapor Deposition." Appl. Phys. Lett. 95, no. 18 (2009): 183105. © 2009 American Institute of Physics

As Published: http://dx.doi.org/10.1063/1.3259415

Publisher: American Institute of Physics (AIP)

Persistent URL: http://hdl.handle.net/1721.1/85955

Version: Final published version: final published article, as it appeared in a journal, conference proceedings, or other formally published context

AIP | Applied Physics Letters

All graphene electromechanical switch fabricated by chemical vapor deposition

Kaveh M. Milaninia, Marc A. Baldo, Alfonso Reina, and Jing Kong

Citation: Applied Physics Letters **95**, 183105 (2009); doi: 10.1063/1.3259415
View online: http://dx.doi.org/10.1063/1.3259415
View Table of Contents: http://scitation.aip.org/content/aip/journal/apl/95/18?ver=pdfcov
Published by the AIP Publishing

All graphene electromechanical switch fabricated by chemical vapor deposition

Kaveh M. Milaninia,[1,a)] Marc A. Baldo,[2,b)] Alfonso Reina,[1,c)] and Jing Kong[2,d)]
[1]*Department of Materials Science and Engineering, Massachusetts Institute of Technology, Cambridge, Massachusetts 02139, USA*
[2]*Department of Electrical Engineering and Computer Science, Massachusetts Institute of Technology, Cambridge, Massachusetts 02139, USA*

(Received 17 September 2009; accepted 14 October 2009; published online 5 November 2009)

We demonstrate an electromechanical switch comprising two polycrystalline graphene films; each deposited using ambient pressure chemical vapor deposition. The top film is pulled into electrical contact with the bottom film by application of approximately 5 V between the layers. Contact is broken by mechanical restoring forces after bias is removed. The device switches several times before tearing. Demonstration of switching at low voltage confirms that graphene is an attractive material for electromechanical switches. Reliability may be improved by scaling the device area to within one crystalline domain of the graphene films. © *2009 American Institute of Physics*. [doi:10.1063/1.3259415]

Power consumption is the major technical problem facing the semiconductor industry today.[1] An important contributing factor is the subthreshold slope of contemporary transistors. This is a measure of the gate electrode voltage swing required to modulate the channel conductance by an order of magnitude. The subthreshold slope influences power consumption by limiting reductions in the supply voltage. Reductions in the supply voltage decrease the maximum possible gate voltage swing and either result in transistors not being fully turned on, yielding slower circuit operation, or transistors not being fully turned off, yielding larger static power consumption.

Recently, it has been proposed that the sharp switching characteristics of nanoelectromechanical (NEM) switches may help reduce power consumption.[2] But reliable NEM switches have not been demonstrated with low voltage operation and low contact resistances.[3–5] One of the leading problems is failure due to irreversible switching, or stiction,[6] which arises primarily from capillary forces between hydrophilic surfaces and short range interactions such as van der Waals forces. The solution to preventing stiction has been either of the following: (i) create structures with large elastic restoring forces,[7] (ii) avoid direct contact and operate in the regime of tunneling,[3] or (iii) coat contacts with an insulating material to prevent stiction.[3] Unfortunately these approaches result in either high operating voltages or low currents in the on state.

Graphene may help overcome stiction and reliability problems in NEMs. Not only does graphene exhibit exceptional electrical and mechanical properties,[8] but graphene is hydrophobic and the weak interactions between stacked graphene sheets and graphene-shells in multiwall carbon nanotubes have already been exploited to create devices such as nanotube memory elements and bearings for nanorotors.[2,9–12] Typically, the deposition of graphene on a surface is performed by mechanical exfoliation of graphene sheets from a highly oriented pyrolytic graphite (HOPG) source.[13] Although this technique has yielded graphene sheets with relatively large dimensions, it may not be applicable to the fabrication of large area devices and it is only compatible with a "bottom-up" fabrication approach.[5] Recently it has been shown that graphene films of near arbitrary size can be grown by ambient pressure chemical vapor deposition (CVD).[14,15] These CVD graphene films consist of multiple domains of single and multilayers of graphene and exhibit many of the qualities of mechanically exfoliated graphene.[14] In addition these films can be transferred to almost any substrate facilitating the use of "top-down" fabrication. In this letter, we present a large area, all CVD graphene switch.

A schematic picture of the all CVD graphene switch is shown in Fig. 1. A flexible top beam of CVD-grown

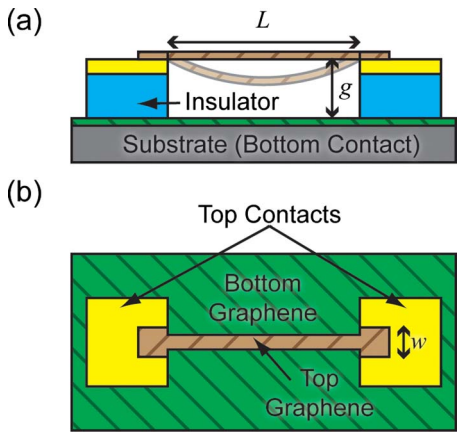

FIG. 1. (Color online) Schematic diagram of an all CVD graphene switch from (a) a cross sectional view and (b) a top view. The device consists of two layers of CVD-grown graphene. The bottom graphene is placed on a conductive substrate which functions as a bottom contact. The top graphene film is patterned into a beam with a length and width of $L=20$ μm and $w=3$ μm, respectively, and suspended above the bottom contact by a gap, $g=500$ nm. The top graphene beam is held in place via two top metal contact electrodes. The switch is activated through the application of a bias between top and bottom contacts.

a)Author to whom correspondence should be addressed. Tel.: 617-519-9783. Electronic mail: kavehm@mit.edu.
b)Tel.: 617-452-5132. Electronic mail: baldo@mit.edu.
c)Tel.: 857-998-9537. Electronic mail: alfonso@mit.edu.
d)Tel.: 617-324-4068. Electronic mail: jingkong@mit.edu.

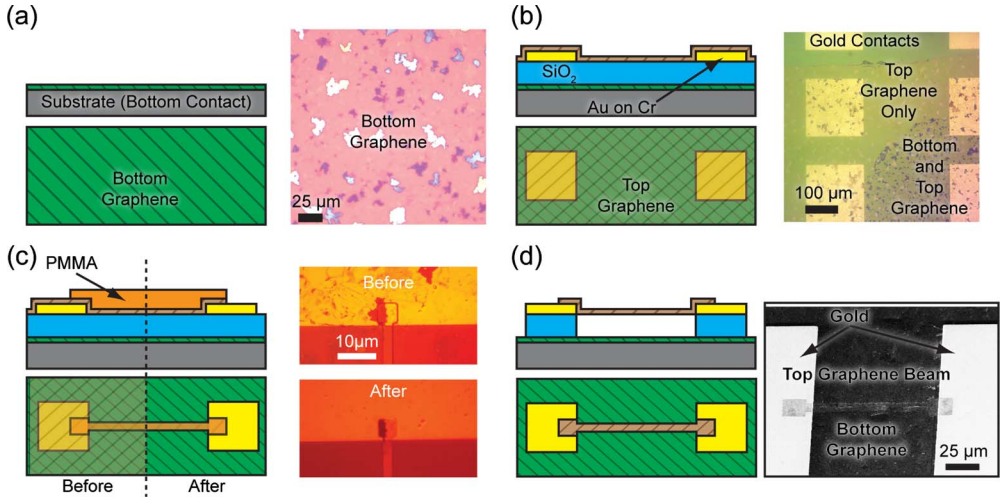

FIG. 2. (Color online) Schematic side and top views [(a)–(d), left], photomicrographs [(a)–(c), right], and scanning electron micrographs [(d), right] of the fabrication process. (a) A large area CVD grown graphene layer is transferred by PMMA transfer onto a highly-doped Si substrate. (b) An insulating silicon dioxide layer is grown using PECVD, gold on chrome contact pads are patterned, and a second graphene layer is transferred on top using the same PMMA transfer method. (c) PMMA is spun on the surface and patterned to create beam structures, this is the "before" state. Using PMMA as an etch mask the pattern is transferred to the top graphene layer using oxygen plasma, this is the "after" state. (d) Finally, PMMA is stripped and the oxide layer is etched away to release the final structure.

graphene is suspended above an inflexible bottom film of graphene. There are three contacts: two top contacts made to either end of the top graphene beam and a bottom contact made to the lower graphene film. The top contacts allow electrical characterization of the flexible top graphene beam. A capacitive force resulting from an applied bias between the top and bottom contacts brings the top beam into electrical contact with the bottom graphene film. When the bias is removed, elastic forces and weak stiction forces allow the top beam to return to its initial position.

The fabrication process is shown in Fig. 2. The graphene films used for this device are grown by ambient pressure CVD on thin films of transition metals.[14,15] Slow cooling ensures that up to 87% of the area is composed of no more than two graphene layers.[16] To form the bottom contact, a CVD graphene layer is transferred onto a highly doped silicon substrate using a poly(methyl methacrylate) (PMMA)-based process previously reported for the transfer of large area graphene films onto arbitrary substrates [Fig. 2(a)].[15] Next, a 500-nm-thick silicon dioxide layer (SiO_2) is deposited using plasma enhanced chemical vapor deposition (PECVD) to define the gap, g. The top contacts, each consisting of an interfacial layer of 7-nm-thick Cr capped by 50 nm of Au, are then patterned on the surface of the SiO_2. A second graphene film is transferred on top of the insulator/contact stack [Fig. 2(b)]. A 500-nm-thick layer of 495 k molecular weight PMMA is spun on the sample to act as a photoresist. Then beams of lengths and widths ranging from $L=5-100$ μm and $w=3-10$ μm, respectively, are photolithographically patterned using a deep ultraviolet (DUV) light source. The beam patterns are transferred to the top graphene film using oxygen plasma etching [Fig. 2(c)],[17] performed with a Plasma Therm Model 790 RIE at an oxygen flow rate of 10 sccm, a chamber pressure of 10 mTorr, a power of 100 W, and an etch time of 3–4 min. The PMMA mask is then dissolved away using acetone. Finally, the regions of the SiO_2 not masked by the top and test electrodes are etched by a combination of dilute hydrofluoric acid and critical point drying [Fig. 2(d)].[18,19] The integrity of the fabricated devices is examined by measuring the current-voltage (I-V) characteristics between the top contacts. This method is employed since the suspended devices are optically transparent and scanning electron microscopy risks damage or contamination of the graphene layers. We observe that many of the larger devices are torn apart in the final step but the thinner, $w<3$ μm, beams remain intact. Similar results have been reported for suspended HOPG-based graphene devices.[18,19]

The electromechanical properties of the double graphene switches are examined by measuring the current between the top and bottom electrodes, while cycling the voltage between 0 and 5 V. Representative I-V characteristics are shown in Fig. 3. In the first sweep from 0 to 5 V, a sharp increase in the current at 4.5 V signals that the top graphene beam has been pulled into contact with the bottom graphene film. The hysteretic behavior as the voltage is swept back to 0 V indicates that the top graphene beam remains in contact with the bottom graphene film until the bias is removed. We suspect that the graphene does not release until either the bias is removed or at extremely low voltages because of weak elastic forces. The nonlinear leakage currents prior to switching

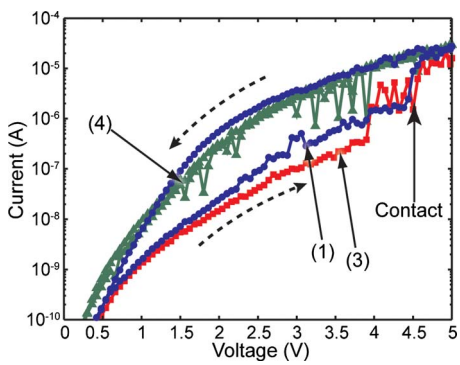

FIG. 3. (Color online) Current-Voltage characteristics between the top and bottom contacts for a $w=3$ μm, $L=60$ μm device showing multiple switching transitions: (1) first scan, (3) third scan (plotted only from 0 to 5 V), and (4), the fourth and final scan.

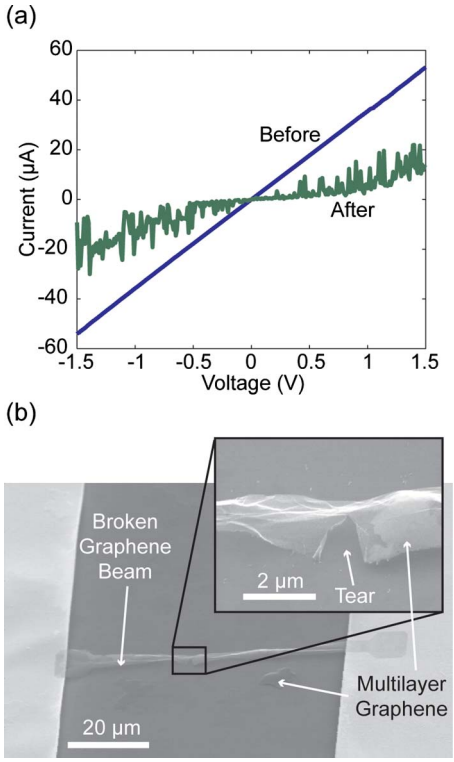

FIG. 4. (Color online) Electrical and physical evidence of mechanical failure in large area CVD graphene switches. (a) I-V data of the graphene beam measured across the top contacts before and after switching measurements. (b) Scanning electron micrograph of a shorted device after testing. Inset is a magnified image of tear in graphene beam. Note that this image is flipped left-to-right relative to Fig. 2(d) (right).

are attributed to conduction through defects, such as pinholes, commonly seen in low temperature PECVD SiO_2.[20] Voltage cycling is repeated several times until the top graphene beam remains in permanent electrical contact with the bottom graphene film. Once this occurs a subsequent I-V measurement shows no hysteretic behavior, as seen in the fourth scan of Fig. 3.

The device failure is caused by a tear in the graphene beam. The I-V data shown in Fig. 4(a) shows a corresponding increase in the resistance of the top graphene beam, as obtained by applying a bias across the top electrodes. The scanning electron micrograph in Fig. 4(b) demonstrates that the torn beam remains in contact with the bottom graphene layer causing the device to short circuit. The onset of the tear is observed in the I-V of a run immediately prior to failure; the third scan in Fig. 3 exhibits large fluctuations in current, starting at 4 V, as the top graphene beam is pulled down.

Similar to previous reports the graphene films exhibit excellent electronic properties,[14,15] the sheet resistance as measured between the top contacts is 900–1100 Ω/sq. In addition, with an average cross-sectional thickness of about 3 nm these films are able to accommodate current densities in excess of 7 kA/cm^2 making them extremely robust electrical conductors. The on-state current is 10 $\mu A/\mu m$ at 5 V and is limited by a contact resistance of <200 kΩ between the top and bottom graphene layers. We expect that the contact resistance is limited by the nonuniform surface of the CVD-grown graphene.

In summary we have demonstrated an electromechanical switch with two CVD-grown graphene electrodes capable of multiple switching at applied biases below 5 V. We suspect that fracture of the suspended graphene beam occurs at a polycrystalline grain boundary. Devices fabricated within a single domain of graphene may exhibit superior reliability.

This work was carried out financially supported by DARPA Grant No. N66001–08–1–2002 and the MARCO Interconnect Focus Center.

[1]International Technology Roadmap for Semiconductors (ITRS), *Design, Semiconductor Industry Association* (SIA, San Jose, 2007).
[2]T. Rueckes, K. Kim, E. Joselevich, G. Y. Tseng, C.-L. Cheung, and C. M. Lieber, Science **289**, 94 (2000).
[3]S. W. Lee, D. S. Lee, R. E. Morjan, S. H. Jhang, M. Sveningsson, O. A. Nerushev, Y. W. Park, and E. E. B. Campbell, Nano Lett. **4**, 2027 (2004).
[4]J. E. Jang, S. N. Cha, Y. Choi, G. A. J. Amaratunga, D. J. Kang, D. G. Hasko, J. E. Jung, and J. M. Kim, Appl. Phys. Lett. **87**, 163114 (2005).
[5]W. W. Jang, J. O. Lee, J.-B. Yoon, M.-S. Kim, J.-M. Lee, S.-M. Kim, K.-H. Cho, D.-W. Kim, D. Park, and W.-S. Lee, Appl. Phys. Lett. **92**, 103110 (2008).
[6]B. Bhushan, *Springer Handbook of Nanotechnology* (Springer, Berlin, 2006).
[7]L. L. Mercado, S.-M. Kuo, T.-Y. T. Lee, and L. Liu, A Mechanical Approach to Overcome RF MEMS Switch Stiction Problem, Piscataway, NJ, USA, May 27-30, 2003 p. 377.
[8]J. S. Bunch, A. M. van der Zande, S. S. Verbridge, I. W. Frank, D. M. Tanenbaum, J. M. Parpia, H. G. Craighead, and P. L. McEuen, Science **315**, 490 (2007).
[9]J. Cumings and A. Zettl, Science **289**, 602 (2000).
[10]A. M. Fennimore, T. D. Yuzvinsky, W.-Q. Han, M. S. Fuhrer, J. Cumings, and A. Zettl, Nature (London) **424**, 408 (2003).
[11]B. Bourlon, D. Christian Glattli, C. Miko, L. Forro, and A. Bachtold, Nano Lett. **4**, 709 (2004).
[12]V. V. Deshpande, H.-Y. Chiu, H. W. C. Postma, C. Miko, L. Forro, and M. Bockrath, Nano Lett. **6**, 1092 (2006).
[13]J. C. Meyer, A. K. Geim, M. I. Katsnelson, K. S. Novoselov, T. J. Booth, and S. Roth, Nature (London) **446**, 60 (2007).
[14]K. S. Kim, Y. Zhao, H. Jang, S. Y. Lee, J. M. Kim, K. S. Kim, J.-H. Ahn, P. Kim, J.-Y. Choi, and B. H. Hong, Nature (London) **457**, 706 (2009).
[15]A. Reina, X. Jia, J. Ho, D. Nezich, H. Son, V. Bulovic, M. S. Dresselhaus, and J. Kong, Nano Lett. **9**, 30 (2009).
[16]A. Reina, S. Thiele, X. Jia, S. Bhaviripudi, M. Dresselhaus, J. Schaefer, and J. Kong, Nano Res. **2**, 509 (2009).
[17]X. Lu, H. Huang, N. Nemohuk, and R. S. Ruoff, Appl. Phys. Lett. **75**, 193 (1999).
[18]X. Du, I. Skachko, A. Barker, and E. Y. Andrei, Nat. Nanotechnol. **3**, 491 (2008).
[19]C. Gomez-Navarro, M. Burghard, and K. Kern, Nano Lett. **8**, 2045 (2008).
[20]S. W. Hsieh, C. Y. Chang, and S. C. Hsu, J. Appl. Phys. **74**, 2638 (1993).